



HAL
open science

Platinum nanocluster growth on vertically aligned carbon nano fiber arrays: sputtering experiments and molecular dynamics simulations.

Pascal Brault, Amaël Caillard, Christine Charles, Rod Boswell, David B. Graves

► To cite this version:

Pascal Brault, Amaël Caillard, Christine Charles, Rod Boswell, David B. Graves. Platinum nanocluster growth on vertically aligned carbon nano fiber arrays: sputtering experiments and molecular dynamics simulations.. Applied Surface Science, 2012, 263, pp.352-356. 10.1016/j.apsusc.2012.09.059 . hal-00752502

HAL Id: hal-00752502

<https://hal.science/hal-00752502>

Submitted on 16 Nov 2012

HAL is a multi-disciplinary open access archive for the deposit and dissemination of scientific research documents, whether they are published or not. The documents may come from teaching and research institutions in France or abroad, or from public or private research centers.

L'archive ouverte pluridisciplinaire **HAL**, est destinée au dépôt et à la diffusion de documents scientifiques de niveau recherche, publiés ou non, émanant des établissements d'enseignement et de recherche français ou étrangers, des laboratoires publics ou privés.

Platinum nanocluster growth on vertically aligned carbon nanofiber arrays: sputtering experiments and molecular dynamics simulations

Pascal Brault^{a,*}, Amaël Caillard^a, Christine Charles^b, Rod W. Boswell^b,
David B. Graves^c

^a*GREMI, UMR7344 CNRS-Université d'Orléans BP 6744, 45067 Orléans Cedex 2, France*

^b*Space Plasma, Power and Propulsion Group, Research School of Physics and Engineering,
The Australian National University, Canberra, ACT 0200, Australia*

^c*Department of Chemical and Biomolecular Engineering, 201 Gilman Hall 1462, University
of California Berkeley, CA 94720-1462 USA.*

Abstract

Sputtered platinum nanocluster growth on previously plasma enhanced chemical vapor deposition - PECVD - grown vertically aligned carbon nanofiber arrays is presented. Experimental cluster size distribution is shown to decrease from the CNF top to bottom, as observed by transmission electron microscopy. Molecular Dynamics simulations are carried out for understanding early stages of Pt growth on model CNF arrays. Especially, sticking coefficients, concentration profiles along CNF wall, cluster size distributions are calculated. Simulated cluster size distribution are consistent with experimental finding. Sticking coefficient decreases against deposition time. The shape of the sticking curve reflects the nanocluster growth process.

Keywords: nanocluster growth; Carbon nanofibers; sputtering deposition; PECVD; molecular dynamics simulation; sticking coefficient

1. Introduction

Deposition and growth of metals nanoclusters on carbon nanofibers is of great interest for many applications such as fuel cell electrodes [1, 2, 3, 4, 5], and more generally as electrocatalytic films [6, 7]. A great amount of experiments have thus been devoted to the manufacture of such devices. Investigation of cluster growth dynamics on complex substrate structures is highly desirable. Targeted experiments are possible using transmission electron spectroscopy but the information is usually very localized and requires statistically significant analyses [8, 9, 10]. Even if valuable information on nanocluster growth can

*Corresponding author

Email address: `Pascal.Brault@univ-orleans.fr` (Pascal Brault)

be deduced from such experiments, this is after a sufficient deposition time, which does not give access to initial steps of growth. Among simulation tools at the atomic scale, Classical Molecular Dynamics is a unique method for exploring detail of atomic processes at surfaces, especially those encountered at the plasma-surface interface where non equilibrium growth phenomena are known to occur [11].

2. Experiments

Plasma sputter deposition of platinum on PECVD grown vertically aligned carbon nanofiber arrays is carried out in an Inductively Coupled Plasma [1, 2, 3]. The plasma is generated by a 13.56 MHz radio frequency powered double saddle antenna placed around the 15 cm diameter glass source tube attached to a diffusion chamber shaped as a cross (55.5 cm x 55.5 cm). Three solenoids surround the source and the diffusion chamber to produce a magnetic field of about 80 G along the vertical axis between the helicon source and the 72 mm diameter substrate holder. The CNF holder can be DC biased and manually rotated and moved along the vertical axis. It is usually placed 18 cm below the plasma source. Pt nanoclusters are grown on the CNF carpets using a -300 V biased Pt target sputtered by ions generated by an argon plasma of pressure and power of 0.5 Pa and 500 W, respectively. Center to center distance between Pt target to CNF substrate is 8.5 cm. A typical view of the CNF carpet without and with grown Pt nanoclusters is shown in figure 1.

Figure 1(a) clearly show that the CNF are vertically aligned and organized as a 2D array with CNF mean diameter of 35 ± 15 nm and length of 1.7 ± 0.35 μ m, mean separation between 100 and 200nm. A controlled amount of $60 (\pm 6) 10^{15}$ Pt atoms per cm^2 ($20 \mu\text{g cm}^{-2}$ of platinum) was sputtered on these CNFs during 4 min. The SEM picture in figure 1(b) show the resulting Pt-CNF structure. Clearly defined nano-sized Pt particles are observed along and around all the CNF (white areas on the micrographs), from the top where the nano-clusters are more prevalent to the bottom where they are more dispersed. The nano-clusters size and density decrease from the top to the bottom of the CNF. This is confirmed by the TEM picture in the inset of Figure 2 which gives the experimental distribution of Pt nanoclusters along the CNF.

3. Molecular Dynamics simulations

Molecular dynamics simulations are carried out on model nanofibers of diameter 9.2 nm (the lower limit of the diameter distribution in Figure 1). On Figure 3 are plotted the model CNFs. The height of the CNFs is 20 nm standing on a square support defining the area of the simulation box. The simulation box

is either a $10 \times 10 \text{ nm}^2$ elementary cell base with 143498 carbon atoms (CNF1) with a height of 20 nm (Fig. 3a) which provides a void fraction between fibers of 34% or a $20 \times 20 \text{ nm}^2$ base with 173677 carbon atoms (CNF2) with a height of 20 nm (Fig. 3b) and 307232 carbon atoms (CNF3) with a height of 40 nm (Fig. 3c) leading to a void fraction of 82 % which is close to the CNF carpet of Figure 1. The heights of the simulation fibers are very small compared to experimentally obtained nanofibers, but for early deposition times, it is not an important factor. Because periodic boundary conditions will be imposed, calculation using an elementary cell is strictly equivalent to perform the calculations on a 2D periodic square array, that can be thus compared to experimental results. The differences between the three simulation boxes are the CNF spacings and heights.

The molecular dynamics simulation intends to solve classical Newton set of equations describing the motion of atoms. This can be written in the form :

$$m_i \frac{\partial^2}{\partial t^2} \vec{r}_i = \sum_{\lambda} \vec{F}_i(\lambda) \quad (1)$$

where m_i is the mass of the i^{th} incoming atom interacting through the forces $\vec{F}_i(\lambda)$. λ stands for both CNF and adsorbed atoms. In principle, the same set of equations for the surface atoms should be applied to the CNF atoms: they interact among themselves and also with adsorbed atoms. In the following, the CNF atoms remain at their initially fixed positions. This is justified here for two reasons: first, true CNF surface is rigid, second, impinging atom energies are well below the carbon displacement energies. Indeed, the initial kinetic energy is randomly selected in a Maxwell distribution at 300 K. This describes conditions for which sputtered atoms are thermalized (kmean kinetic enegy is around 0.03 eV corresponding to 300 K vapor) during the transport between the Pt target and the CNF substrate. This is the case for the present experiments ($d=8.5 \text{ cm}$ and $P = 0.5 \text{ Pa}$). A crucial problem in Molecular Dynamics is to find a way for dissipating energy through the solid for allowing bonding to the surface. A method including a frictional term issued from Sommerfeld theory [12, 13] is presently used: if at the ongoing time step $\vec{F} \cdot \vec{v} < 0$ (\vec{F} is the total force exerted on the considered atom), \vec{v} is the current velocity), then the following Langevin-like equation is solved,

$$m_i \frac{\partial^2}{\partial t^2} \vec{r}_i = \sum_{\lambda} \vec{F}_i(\lambda) - \mu \vec{v} \quad (2)$$

instead of Eq. (1). Following [12], the friction coefficient can be written as:

$$\mu = m\alpha \frac{T_i - T_s}{T_i} \quad \text{and} \quad \alpha = \frac{\Theta_D T_e L n e^2 k_B Z}{2 m_e \kappa \epsilon_F} \quad (3)$$

With Θ_D being the Debye temperature, T_s the substrate temperature, L the Lorentz number, n the free electron density, e electron charge, k_B the Boltzmann constant, Z metal oxidation state, m_e the electron mass, κ the thermal

conductivity, ϵ_F the Fermi energy and T_i the kinetic temperature (data from ref. [14]). It should be noticed that $\tau = \frac{1}{\alpha}$ is the relaxation time, *i.e.* the mean time during which the impinging atoms release their kinetic energy to the substrate. For Pt τ is calculated to be 1.17 picosecond according to Eq.(3). For simulating a deposition atoms need to be released one after each other with a reasonable time delay Δt : *i.e.* sufficient for allowing thermal relaxation of the already deposited atoms, which do not mean they do not move. In other words, the simulations can be thought of as following the short (~ 1 ps) impact time for each individual atom impacting the surface, then after the excess kinetic energy is dissipated/removed, another atom is brought to the surface. The 'true' simulation 'time' is then related to the experimental flux. Thus $\Delta t \sim \tau$ and is chosen equal to 0.8 ps. Increasing this time delay does not affect the results. In each simulation, 10000 Pt atoms are injected. The integration time is $dt=0.4$ fs.

Implementing suitable interatomic potentials is certainly the most important issue in molecular dynamics calculations [11, 15, 16, 17]. For describing platinum interactions, we use a tight-binding potential in the second moment approximation (TB-SMA)[18]. Such a potential is non pairwise in the sense that if atom i interacts with atom j , the atoms surrounding atom j are explicitly taken into account. The TB-SMA force equation acting on atom i due to atom j surrounded by atoms k , can be written as :

$$\begin{aligned} \vec{F}_i(\text{Pt} - \text{Pt}) = & \sum_{j \neq i, r_{ij} < r_c^{TB}} \left\{ 2Ap \exp \left[-p \left(\frac{r_{ij}}{r_0} - 1 \right) \right] \right. \\ & \left. - \frac{\xi q}{r_0} \left[\frac{1}{\sqrt{E_i^b}} + \frac{1}{\sqrt{E_j^b}} \right] \exp \left[-2q \left(\frac{r_{ij}}{r_0} - 1 \right) \right] \right\} \frac{\vec{r}_{ij}}{r_{ij}} \end{aligned} \quad (4)$$

with

$$E_i^b = \sum_{j \neq i} \exp \left\{ -2q \left(\frac{r_{ij}}{r_0} - 1 \right) \right\} \quad (5)$$

and

$$E_j^b = \sum_{k \neq j} \exp \left\{ -2q \left(\frac{r_{jk}}{r_0} - 1 \right) \right\} \quad (6)$$

where r_0 is the first neighbor distance. For platinum $r_0 = 0.277$ nm. The interaction is cut off at $r_c^{TB} = 2.5r_0$ (which includes neighbors up to the 5th). Note the potential used here [18] is defined up to the 5th neighbor. r_{ij} is the interatomic distance between i and j atoms. A, ξ, p, q , are the TB-SMA parameters, respectively equals to; 0.2975 eV, 2.695 eV, 10.612, 4.004 [18]. For interactions with carbon atoms, we used a Lennard-Jones (LJ) 12 - 6 potential issued from fitting Pt interaction with graphite using Sutton-Chen potential

[19]. The force thus becomes,

$$\vec{F}_i(\text{Pt} - \text{C}) = 24 \varepsilon_{\text{Pt}-\text{C}} \sum_j \left\{ 2 \left[\frac{\sigma_{\text{Pt}-\text{C}}}{r_{ij}} \right]^{12} - \left[\frac{\sigma_{\text{Pt}-\text{C}}}{r_{ij}} \right]^6 \right\} \frac{\vec{r}_{ij}}{r_{ij}^2} \quad (7)$$

with $\varepsilon_{\text{Pt}-\text{C}} = 0.022$ eV and $\sigma_{\text{Pt}-\text{C}} = 0.2905$ nm. The equations of motion are solved using the Verlet velocity algorithm [20]. A link-cell list is used to speed-up the computations in conjunction with Verlet lists for which radius $r_v = 2.7r_0$ [15, 16].

4. Results and discussion

The information which can be simply retrieved from MD simulation are snapshots at given deposition times. Figure 4 show the snapshots for 10000 Pt atoms launched onto CNF1, CNF2 and CNF3 substrates. First of all, MD simulated deposition leads to nanocluster Pt growth on the CNF surface. Some interesting features can be highlighted. Comparison between Figures 4(a) and (b) shows that the effect of CNF spacing is to reduce the diffusion or at least the access along the CNF wall surface. Moreover, the Pt density on the top of the CNF is increased when reducing the spacing. Increasing the CNF height (CNF3) does reduce cluster growth at the fiber bottom: in Fig. 4(c), the CNF3 is entirely decorated, and the base also exhibits cluster growth. This comes from atoms having nearly vertical trajectories, or having reflection on neighboring CNF, as a result of boundary conditions.

We can also calculate the evolution of the sticking coefficients versus the deposition time or equivalently versus the launched atom number (Figure 5). The general trend is the sticking coefficient [21] is decreasing in the course of the deposition. Because the surface is disordered at the atomic scale, the clusters are so much organised and adsorption sites are not efficiently binding. The sticking sites are then not easily reached despite the high cohesive energy of platinum. Moreover the low Pt-C bond energy does not favor the diffusion to existing cluster edges for sticking and evaporation during diffusion on free carbon surface is also possible.

The number of atoms trapped on the nanofiber wall surfaces is increased when the CNF spacing is enlarged. For the smallest CNF spacing (CNF1) the drop of sticking coefficient is very pronounced. This can be correlated to the concentration profile displayed in Figure 6(a) which shows the highest degree of concentration on the upper part of CNF1. So the impinging atom have a lower possibilities to travel between columns and find a stable adsorption site. Sticking coefficient is expected to converge towards a stationary value of 0.3. When increasing CNF spacing (edge to edge distance) from 0.8 nm up to 11.8 nm),

the sticking coefficients exhibit a more different evolution. For both heights (20 and 40 nm, Fig 5(b) and (c)), the sticking coefficient is almost constant (about 0.8) up to 4000 injected atoms. This is consistent with cluster growth and precursor kinetics [22, 23]. Above $4 \cdot 10^3$ injected atoms a decrease is observed, but no stationary state is reached, despite an already large amount of adsorbed species. For 10^4 injected atoms, the sticking coefficient remains high (around 0.6) compared to deposition on CNF1. Moreover, the sticking coefficient is high for the highest spacing between CNF. Moreover, concentration profiles (Fig. 6) exhibit a decrease along the CNF wall surfaces. These concentration profiles $\rho(z)$ are fitted with a stretched gaussian function $\rho(z) \propto A \exp \left[-\frac{(z - z_0)^{2+\theta}}{\lambda} \right]$ (see red line in Fig. 6), solution of a generalized diffusion equation [24]. θ is a parameter characterizing the diffusing medium, A being the pre-exponential factor and λ the spreading of the stretched gaussian function. It should be noticed that the "porosity exponent" θ is of the same order as the one for Pt deposition/diffusion into a carbon sphere stacking i.e. $\theta \approx -1.5$ [24], which is a more tortuous medium.

All this suggests that Pt atoms have more possibilities for reaching a stable site or an already existing cluster by allowing a more efficient transport when increasing the spacing between fibers. Moreover, increasing the fiber height does not change the coverage along the CNF wall while the concentrations profiles do (Fig. 6(b) and c)). The spreading factor λ is increasing when increasing height and fiber spacing : $\lambda = 1, 6, 8$ in Fig. 6(a) to (c).

Finally, the cluster size distribution are calculated (Fig. 7) and are clearly different depending on the considered CNF substrate. The most regular distribution is obtained for deposition onto CNF3, Fig7(c). The asymmetric tail spreading towards larger cluster size is due to the regularly decreasing cluster size along the CNF length from top to bottom. This is consistent with the observed Pt nanocluster distribution displayed on Fig. 2. Keeping in mind that molecular dynamics describe early deposition time and the picture of Fig. 2 is taken at longer time, comparison remains valid if the large time experimental cluster distribution truly reflect early time one. Which is certainly the case here [24].

5. Conclusions

Molecular Dynamics simulations of Pt deposition onto CNF are carried out. They show, similarly to the results of the sputter deposition experiments, that simulated deposition leads to nanocluster growth, for which characteristics depend on CNF spacing and height. The concentration profiles fully extend along the CNF height if spacing is sufficient, otherwise the concentration profile is localized on the upper part of the CNF. Agreement between experiments and

simulations is also obtained with diffusion equation solutions, especially the "porosity" exponent. The MD calculated cluster size distribution on CNF3 is consistent with the experiments. The huge difference in CNF height between experiments and simulations plays no role as far as early time deposition is concerned. Short time molecular dynamics simulations can be compared to experiments at longer times if a scaling is known.

References

- [1] A. Caillard A, C. Charles, R. Boswell, P. Brault, C. Coutanceau, *Appl. Phys. Lett.* 90 (2007) 223119
- [2] A. Caillard, C. Charles, R. Boswell, P. Brault, *Nanotechnology* 18 (2007) 305603
- [3] A. Caillard, C. Charles, R. Boswell and P. Brault, *J. Phys. D* 48 (2008) 185307
- [4] N. Soin, S.S. Roy, L. Karlsson, J.A. McLaughlin, *Diamond & Related Materials* 19 (2010) 595-598
- [5] K. Prehna, R. Adelung, M. Heinen, S. P. Nunes, K. Schulte *Journal of Membrane Science* 321 (2008) 123-130
- [6] T.-F. Hsieh, C.-C. Chuang, Y.-C. Chou, C.-M. Shu, *Materials and Design* 31 (2010) 1684-1687
- [7] Y. Liu, J. Chen, W. Zhang, Z. Ma, G. F. Swiegers, C. O. Too, and G. G. Wallace, *Chem. Mat.* 20 (2008) 2603
- [8] P. Brault, A. L. Thomann, C. Andreazza-Vignolle, *Surf. Sci.* 406 (1998) L597-L602
- [9] P. Brault, A.-L. Thomann, C. Andreazza-Vignolle, P. Andreazza, *Eur. Phys. J. Appl. Phys.* 19(2002) 83-87
- [10] P. Andreazza, C. Andreazza-Vignolle, J. P. Rozenbaum, A.-L. Thomann, P. Brault, *Surf. Coat. Technol.* 151-152, 122-127 (2002)
- [11] D. B. Graves, P. Brault, *J. Phys. D: Appl. Phys.* 42 (2009) 194011 (27pp)
- [12] Q. Hou, M. Hou, L. Bardotti, B. Prevel, P. Melinon, and A. Perez, *Phys. Rev. B* 62 (2000) 2825
- [13] C. P. Flynn and R. S. Averbach, *Phys. Rev. B* 38 (1988) 7118
- [14] C. Kittel, *Introduction to solid state physics*, (Wiley & sons, New York, 1996)
- [15] M. P. Allen, D. J. Tildesley, *Computer Simulation of Liquids* (Clarendon Press, Oxford, 1987)

- [16] D. Frenkel, B. Smit, Understanding Molecular Simulations (Academic Press, New York, 1996)
- [17] D. C. Rapaport, The Art of Molecular Dynamics Simulation (Cambridge University Press, 1998)
- [18] F. Cleri, V. Rosato, Phys. Rev. B 48 (1993) 22
- [19] S. Y. Liem et K. Chan, Surf. Sci. 328 (1995) 119
- [20] W. C. Swope, H. C. Andersen, P. H. Berens and K. R. Wilson, J. Chem. Phys. 76 (1982) 637
- [21] The use of terms sticking and sticking coefficients remains controversial. The most used term is "sticking", and we will use it. Nevertheless, a more appropriate term here is "condensation coefficient". In principle sticking is used in molecular adsorption (either dissociative or not) leading to a saturation coverage, at which the sticking has decreased to zero (as in Langmuir adsorption) and which does not allow further growth at all. "Condensation", means that incoming particles accommodates at the surface with a given probability, which might depend on the amount of already adsorbed species. This process does not lead to any saturation coverage, allowing thin film growth with a thickness depending on deposition time (linearly in most situation).
- [22] P. Brault, H. Range, J. P. Toennies, J. Chem. Phys. 106 (1997) 8876 - 8889
- [23] P. Brault, H. Range, J. P. Toennies, Ch. Wll, Zeitschr. Phys. Chem. 19 (1997) 1-17
- [24] P. Brault, Ch. Josserand, J.-M. Bauchire, A. Caillard, Ch. Charles, R. W. Boswell, Phys. Rev. Lett. 102 (2009) 045901

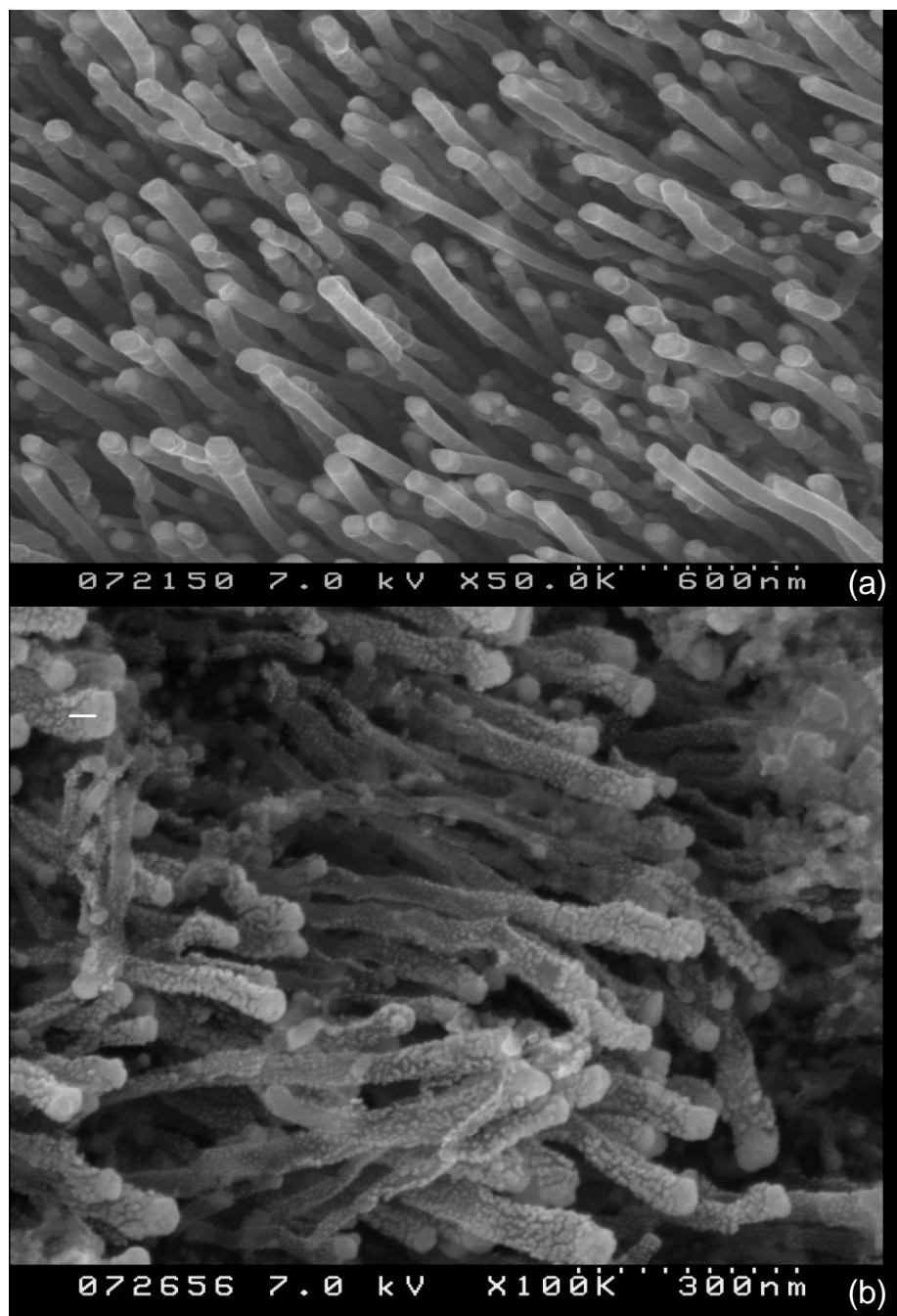


Figure 1: Scanning Electron Microscopy top view of a carbon nanofiber array (a) before Pt deposition (b) after Pt deposition (Pt clusters are visible as white areas)

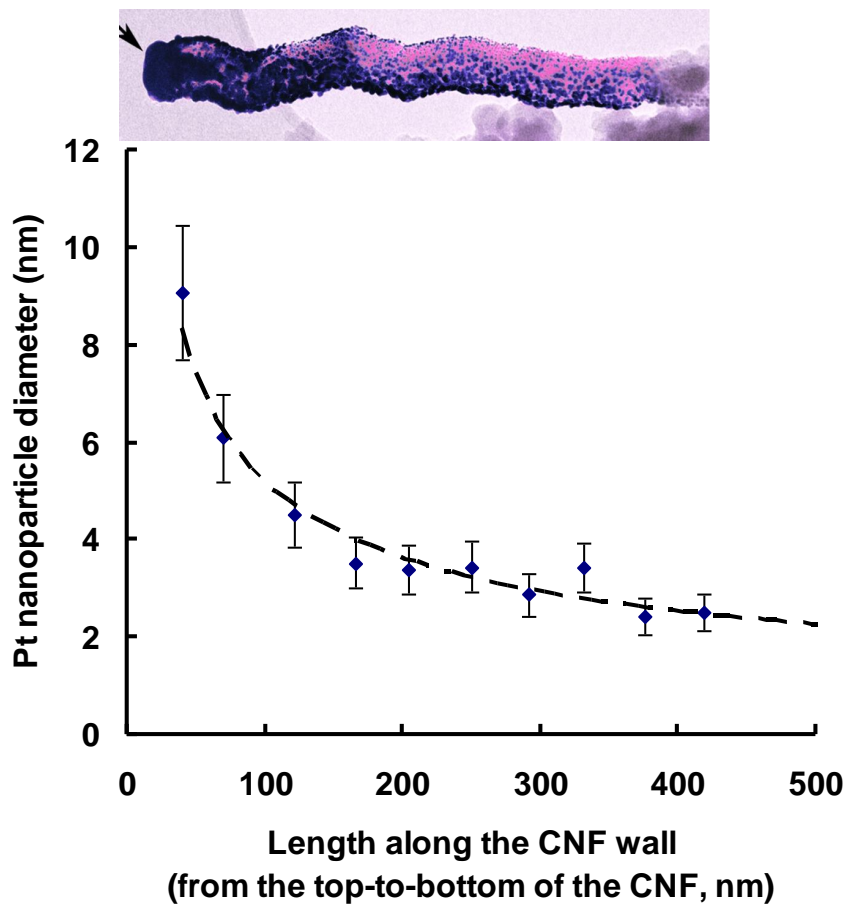


Figure 2: Transmission Electron Microscopy of a Pt "decorated" carbon nanofiber and the corresponding plot of the mean diameter along the CNF length. Pt cluster are dark areas and the arrow on the left indicates the top part of CNF exposed to the Pt flux. The dashed line is for eye guiding

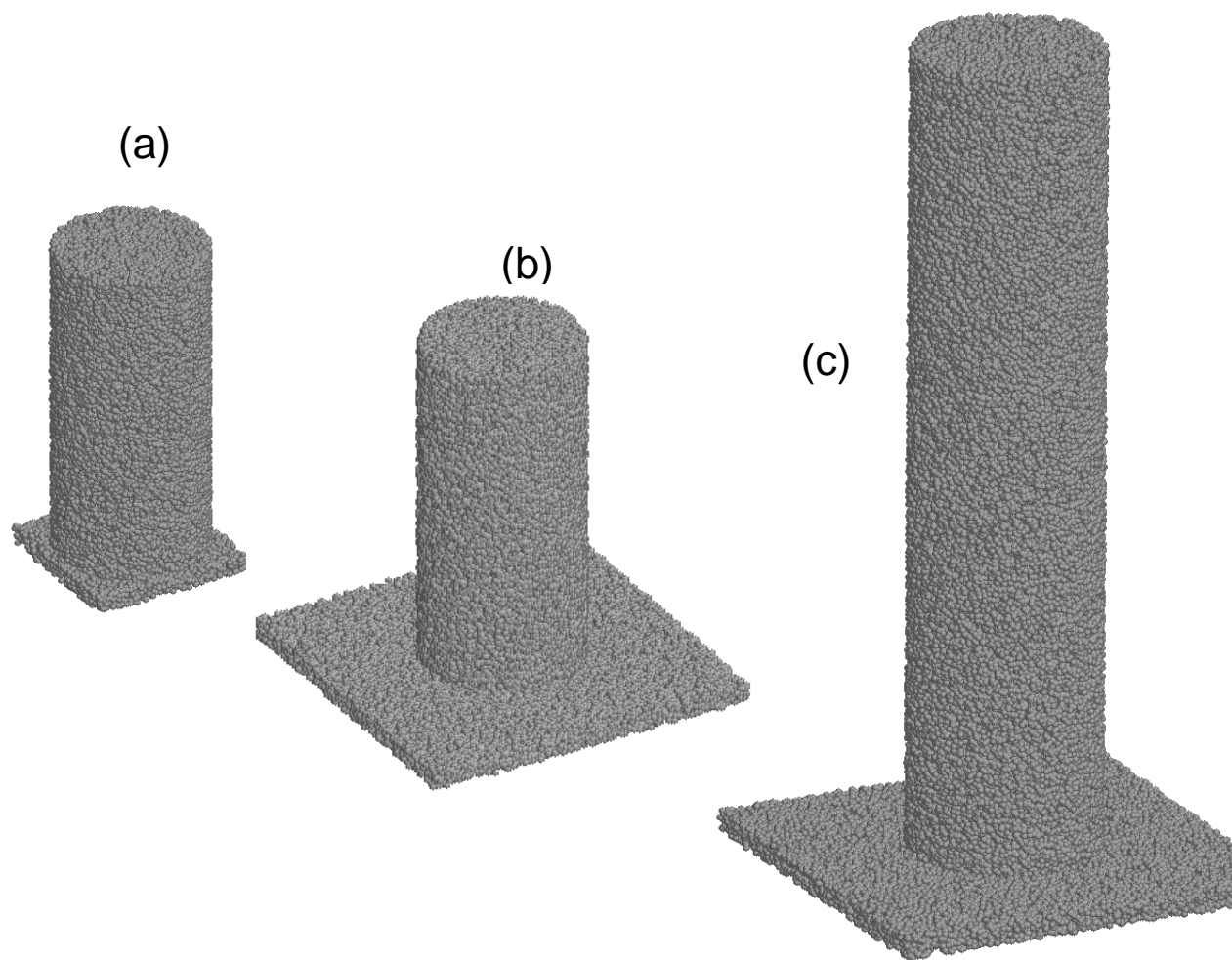


Figure 3: The three model CNF serving as support for Pt deposition. Diameter is 9.2 nm (a) CNF1: substrate is $10 \times 10 \text{ nm}^2$ and height is 20 nm (b) CNF2: substrate is $20 \times 20 \text{ nm}^2$ and height is 20 nm (c) CNF3: substrate is $20 \times 20 \text{ nm}^2$ and height is 40 nm. The spacing (edge to edge distance) between CNF in the equivalent square array, as resulting from periodic boundary conditions is 0.8 nm for CNF1 and 11.8 nm for CNF2 and CNF3

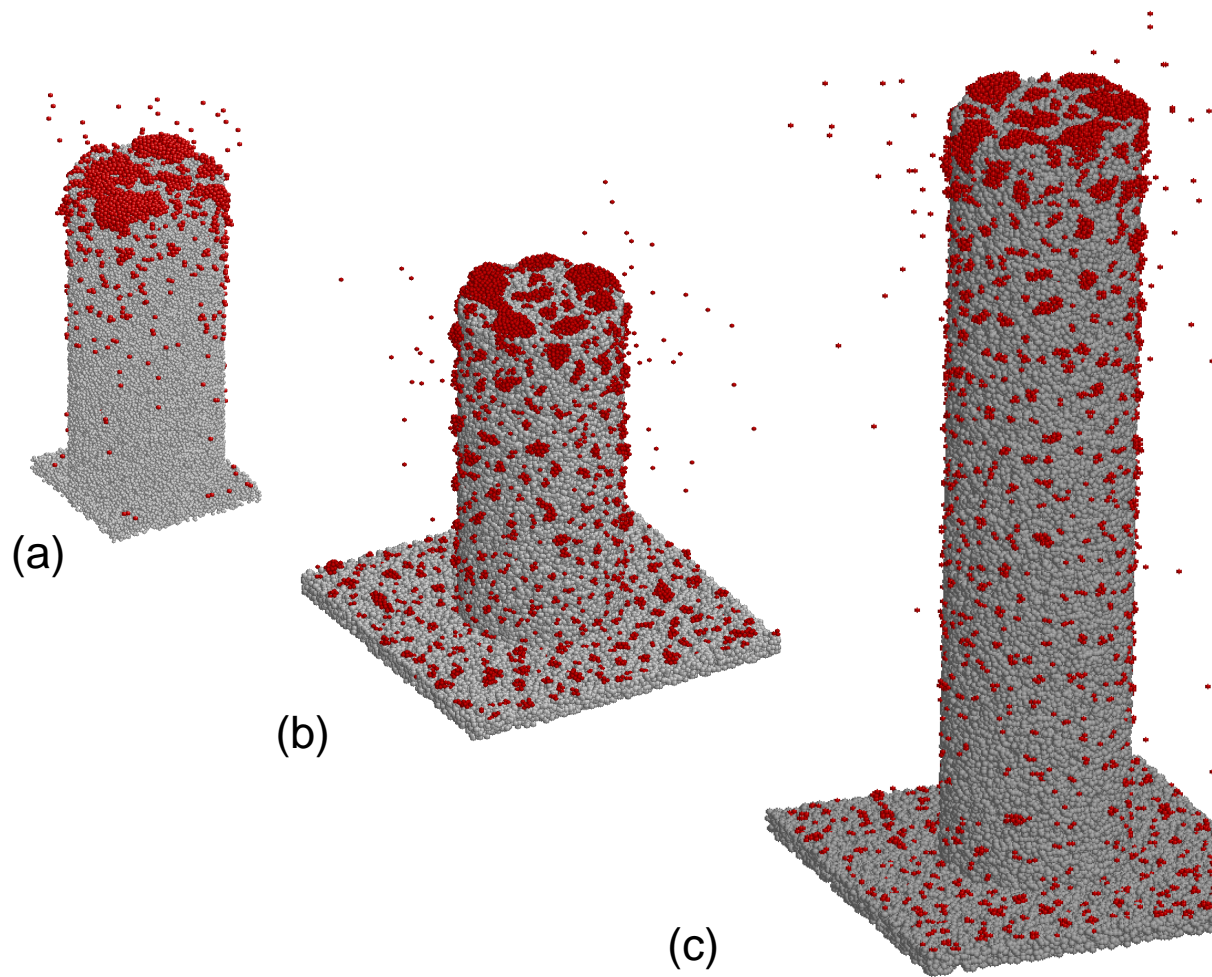


Figure 4: Snapshots of Pt deposited on (a) CNF1 10000 atoms launched, 3149 adsorbed; (b) CNF2: 10000 atoms launched, 5982 adsorbed; (c) CNF3: 10000 atoms launched, 6282 adsorbed

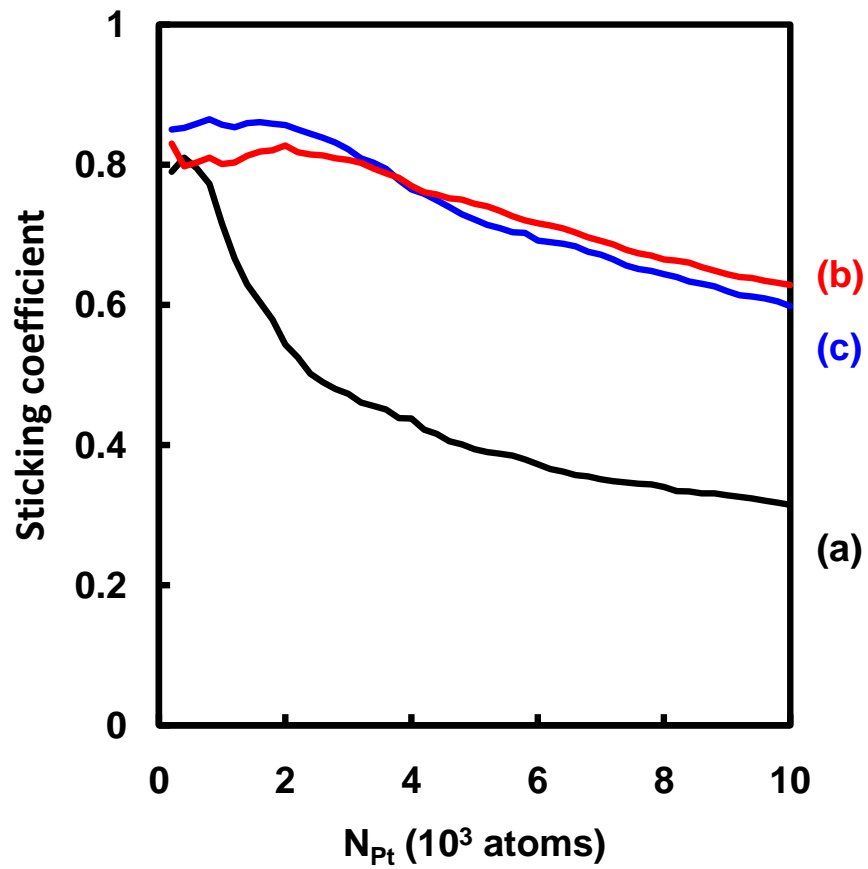


Figure 5: Sticking coefficient evolution vs injected Pt atoms number (a) on CNF1; (b) on CNF2; (c) on CNF3

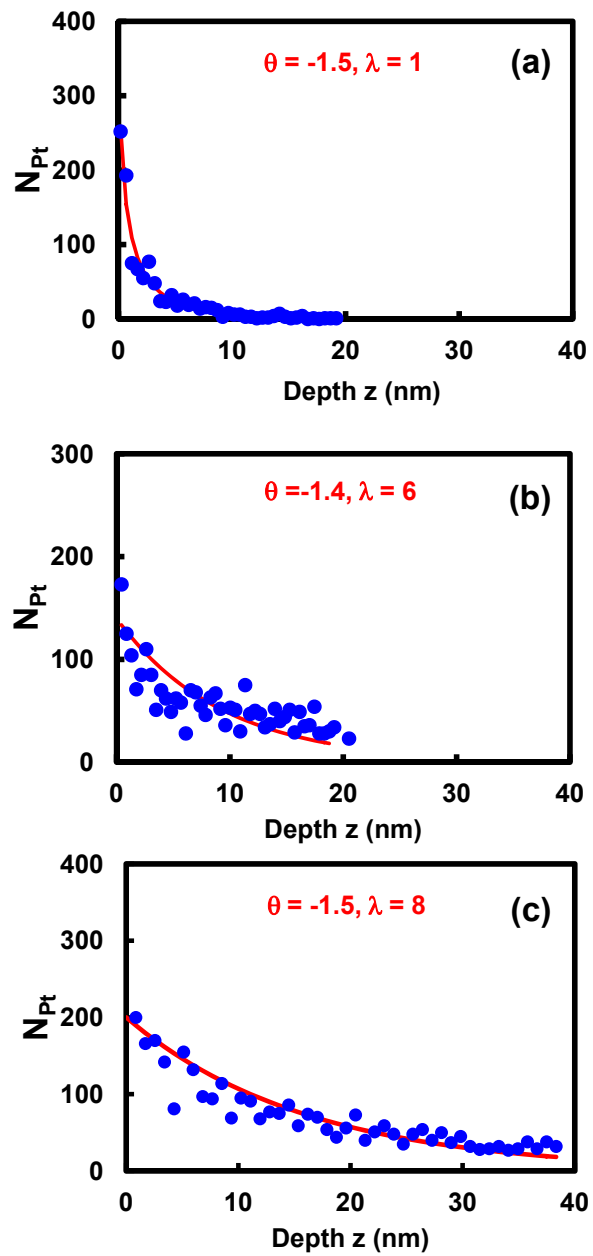


Figure 6: Concentration profiles along the fiber walls (a) on CNF1; (b) on CNF2; (c) on CNF3. the red line is the fitting stretched gaussian function for which θ is a relevant parameter (see text)

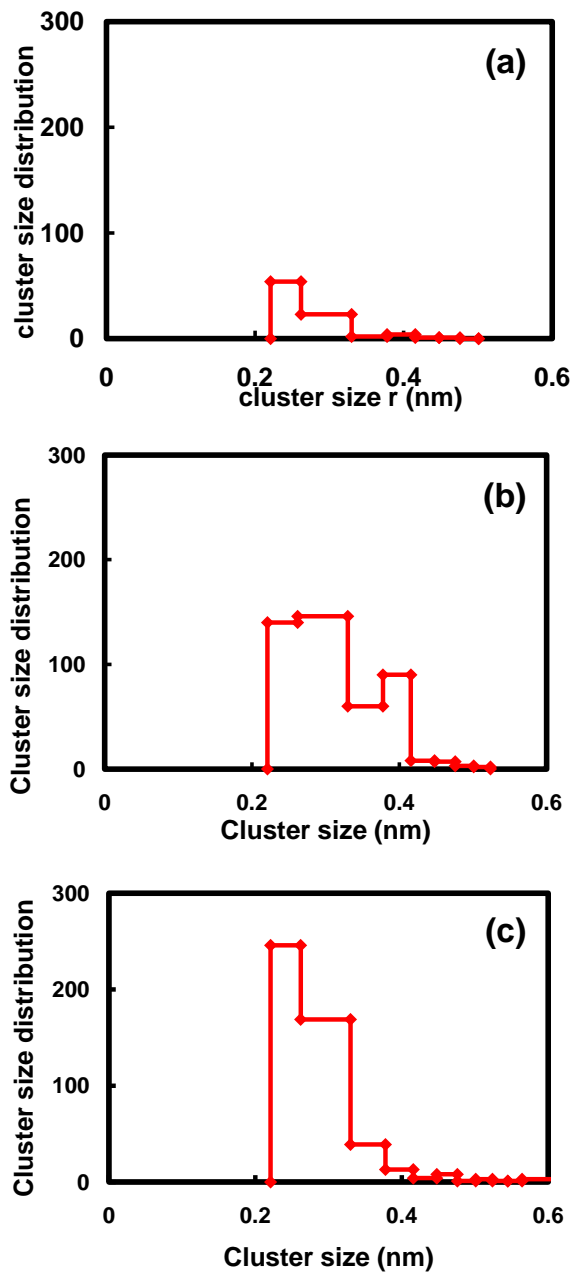


Figure 7: Cluster size distributions. Cluster with 1 to 3 atoms and single large clusters ($n_i > 50$) are excluded (a) on CNF1; (b) on CNF2; (c) on CNF3